Fabrication of TiO_2 Micropatterns on Flexible Substrates by Vacuum-ultraviolet Photochemical Treatments

*Cheng-Tse Wu, Ahmed I. A. Soliman, Yudi Tu, Toru Utsunomiya, Takashi Ichii, Hiroyuki Sugimura**

Cheng-Tse Wu. Author 1, Dr. Ahmed I. A. Soliman. Author 2, Dr. Yudi Tu. Author 3, Dr. Toru Utsunomiya. Author 4, Dr. Takashi Ichii. Author 5, Prof. Hiroyuki Sugimura. Corresponding Author*
Department of Materials Science and Engineering, Kyoto University, Yoshida-Honmachi, Sakyo-ku, Kyoto 606-8501, Japan.
E-mail: sugimura.hiroyuki.7m@kyoto-u.ac.jp

Dr. Ahmed I. A. Soliman. Author 2
Chemistry Department, Faculty of Science, Assiut University, Assiut 71516, Egypt.

Keywords: Titanium dioxide; 172 nm Vacuum-ultraviolet; Photochemistry; Titanium acetylacetonate; Micropatterning

ABSTRACT

TiO_2 micropatterns have received great attention for application of photocatalysis, electronics and optoelectronics. Formation of such micropatterns on polymer substrates is of importance in flexible device fabrication. Vacuum ultraviolet (VUV) oxidative treatment applied on metalorganic precursor gel films serves as a strategy to fabricate metal oxide films on heat-sensitive substrates such as polymers. Here, 172 nm VUV oxidative treatment through a photomask is used to directly convert the titanium metalorganic precursor films into TiO_2 patterns without further heat-annealing. In comparison to the commonly used alkoxide-based precursors, titanium acetylacetonate (TAA) proves to be an appropriate precursor due to its chemical stability in an ambient environment. With this precursor, clear removal of untreated precursor gels is achieved, resulting in well-defined amorphous TiO_2 micropatterns with a minimum feature of 1 μm and a small edge roughness less than ~4%. The innovativeness arises from the one-step VUV photochemical conversion in the whole ambient conditions, which largely reduces complex processes *e.g.* nitrogen-filled glovebox or post-heat treatments. High-quality amorphous TiO_2 micropatterns can be applied to device fabrication of solar cells and

memories. This patterning approach highlighting TiO_2 can be also extended to other metal oxides, which has great potential in surface and device processing.

1. Introduction

Titanium dioxide (TiO_2) has attracted tremendous attention on its unique photocatalytic, photovoltaic, electronic and optoelectronic properties.[1–4] The fabrication techniques of TiO_2 arrays and patterns on substrates are important in the large-area formation of integrated electronics,[5] memories,[6] solar cells,[7] photocatalysis,[8] sensors,[9,10], *etc*. Approaches for TiO_2 thin films including sputtering,[11] sol-gel[12] and chemical vapor deposition[13] could be used to fabricate TiO_2 patterns on inorganic substrates with the assist of photoresist. These methods were conducted in severe reaction conditions *e.g*. high temperature, and they were usually not applicable to polymer substrates. For flexible devices fabrication, new patterning methods, which can be processed in milder conditions and adaptable to flexible polymer substrates, are increasingly required.[14] For example, liquid phase deposition (LPD) was proposed as a useful approach for preparing TiO_2 thin films and micropatterns in mild conditions. In this method, the reaction occurred in a liquid solution at room temperature. A soluble titanium precursor hydrolyzed to form titanium complex ions and condensed to form TiO_2 precipitation.[15,16] Polymer substrates or silicon substrates covered with self-assembled monolayer (SAM) were patterned by UV photolithography to generate affinity-patterns, thus the TiO_2 precipitation on less-affinity regions could be selectively removed to form patterns. Based on this method, TiO_2 micropatterns were successfully fabricated on polymer substrates[17] as well as silicon substrates.[18] However, this method suffered from poor precision since the lift-off process could not precisely remove the TiO_2 on the less-affinity regions.

Photolithographic patterning techniques, which can also be conducted in mild conditions, provide new possibilities for the formation of TiO_2 patterns. Vacuum ultraviolet (VUV, 172 nm, Xe_2 excimer lamp) light is strongly absorbed by O_2, which forms active oxygen species such as

ozone and atomic oxygen.[19–25] VUV light and the active oxygen species (VUV/(O)) could directly dissociate titanium alkoxide precursors to form amorphous TiO_2 thin films.[19,20] However, such titanium alkoxide precursors are not suitable for operation under an ambient atmosphere because they react with water molecules and the resulting hydrolyzed products are insoluble in common solvents. For micropatterning, how to choose a precursor with stable ligands is a key issue related to whether the precursor gels can be clearly removed from the undesired regions. Among the ligands for metalorganic precursor, acetylacetonate is fairly stable in ambient air because its β-diketone structure chelates to the center metal atom and suppresses the hydrolysis and polymerization reactions.[26,27] This acetylacetonate chelating structure can be dissociated by UV or deep UV irradiation, and the irradiated gels were converted to insoluble hydrolyzed products, which could be further annealed to form metal oxides by heat processes.[26,28] Inspired by these, we expect that a VUV oxidative treatment (VUV/(O)) applied on an acetylacetonate-based precursor gel film can directly form metal oxide micropatterns.

In this work, we reported a 172 nm VUV oxidative treatment (VUV/(O)) approach to fabricate TiO_2 micropatterns on a cyclo-olefin polymer (COP) substrate. Titanium acetylacetonate (TAA) was proved to be as an appropriate precursor since it was stable in an ambient environment even after it was exposed to air for 2 h. Photochemical reaction of TAA was characterized by Fourier transform infrared spectroscopy (FTIR) and X-ray photoelectron spectroscopy (XPS) to confirm the formation of TiO_2. The patterning fabrication of TiO_2 was conducted by VUV/(O)-treatment through a photomask, as illustrated in **Figure 1**. The precursor gels on the irradiated regions were converted into insoluble TiO_2 films, then the untreated precursor gel films were washed away by a common solvent to leave TiO_2 patterns. The resulting micropatterns were characterized by optical microscopy, scanning electron microscopy and energy-dispersive X-ray spectrometry (SEM-EDX), and transmission electron microscopy (TEM). As the previously reported, such VUV-generated TiO_2 were not crystalline at this stage.[19,20] This should be a major drawback of the present VUV/(O)-patterning strategy

since the TiO_2 films usually need to be crystallized to obtain good electronic and optoelectronic behaviors.[29] However, there are some examples of photo-induced crystallization from amorphous TiO_2 to rutile. A direct process was reported to convert titanium alkoxide thin films into rutile TiO_2 thin films by irradiating ArF excimer laser.[30] Another example was also reported that a rutile shell was obtained by irradiating amorphous TiO_2 particles using a xenon arc lamp.[31] These provide possibilities to achieve crystallization without high-temperature annealing. By combining with the adequate processes of photo-crystallization, our amorphous VUV/(O)-fabricated TiO_2 micropatterns could be converted into rutile structure in low-temperature conditions to meet a wider range of requirements of device fabrication. Although the as-prepared TiO_2 micropatterns by our method were amorphous in the present stage, these amorphous TiO_2 thin films and micropatterns can be instantly applied to academic and industrial application including sensors,[32] resistive random access memories,[33–36] solar cell elements[37,38] and photovoltaic materials.[39] Amorphous TiO_2 also attracted attention by demonstrating its photo-activities.[40,41] In the final part, we demonstrated an example application of the resulting amorphous TiO_2 patterns, that is, photo-metallization of copper on them to form metal patterns.

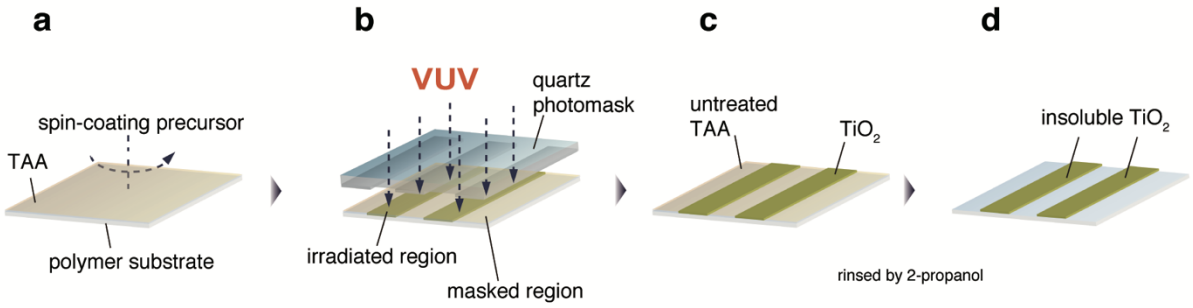

Figure 1. Scheme illustrating VUV/(O) lithographic patterning with quartz photomask and the formation of TiO_2 micropatterns. (a) TAA precursor is spin-coated on the substrate. (b) TAA gel films are treated by VUV/(O) through a photomask. (c) TAA gels in the irradiated region are converted into TiO_2. (d) By 2-propanol rinsing, the untreated precursor gels are washed away, forming TiO_2 patterns on the substrate.

2. Results and Discussion

2.1. VUV/(O)-oxidation of TAA

VUV/(O) photochemical reaction was reported to convert titanium precursors to TiO_2 by removing the organic moieties. To observed the VUV/(O)-induced photo-oxidation reaction of TAA precursor gels, the elimination of the organics could be monitored by observing the IR absorption bands related to acetylacetonate ions. TAA gel films spun on a non-doped Si substrate were first characterized by transmittance-mode FTIR. The chemical composition of TAA gel films were confirmed to be stable in ambient air for 2 h (**Figure S1**), showing that TAA is more stable than those previously reported titanium precursors, *e.g.*, titanium alkoxides.[20,27] The FTIR spectra of TAA gel films on both Si and COP substrates were measured with various VUV/(O)-irradiation time, as shown in **Figure 3**. For clearly judging the chemical changes of TAA after VUV/(O)-treatments, TAA was spin-coated on Si substrates, and the IR absorption bands of the TAA gels were measured after various VUV/(O)-irradiation time. The FTIR measurements were conducted by using the transmittance-mode, thus the Si-substrate-related signals could be successfully subtracted. The IR absorption peaks and bands from the carbon-related vibrations of as-spun TAA gel films were observed as described below. In the chemical forms of CH_x species, the absorption bands at 2970, 2930, 2865 cm^{-1} corresponded to C–H stretching vibrations. The absorption band at 1190-1124 cm^{-1} was due to C–H in-plane bending. The absorption bands at 1585 cm^{-1} and 1524 cm^{-1} were characteristic vibration frequencies from the conjugated C=O and C=C of the acetylacetonate ligands bonded to Ti. The absorption bands at 1383 cm^{-1}, 1279 cm^{-1}, and 1010 cm^{-1} were attributed to CH_3 deformation, CC stretching + CCH_3 stretching, and CH_3 rocking, respectively, which phenomena were due to vibrations from the alkyl structures of the acetylacetonate groups.[27,42–44] The absorption bands corresponding to C–H related vibrations vanished in the first 10 min of irradiation. Strong bands

associated with C=O and C=C vibrations largely decreased in the first 10 min, and mostly disappeared after 2 h of irradiation. These suggested that the VUV/(O)-treatment removed the organic moieties of TAA.

After confirming that the organics in TAA gel films can be cleanly removed by VUV/(O), such VUV/(O)-oxidation of TAA was conducted on our target polymer substrates – COP, and the elimination of the organics in TAA gels was also investigated by using FTIR. Since the detection light in the wavelength of 1500-1400 cm^{-1} cannot penetrate the 188-μm-thick COP substrates,[45,46] the transmittance-mode was no more practicable. The FTIR measurement for TAA gel films spun on COP substrates was conducted by using attenuated total reflection mode (ATR-mode), as shown in **Figure 3b**. However, in the obtained FTIR spectra by ATR-mode, the subtraction of substrate-related signals is difficult due to variation of light penetration depth into the substrates.[47] Therefore, we demonstrated the FTIR spectra without subtraction of substrate-related signals. Before spin-coating the TAA precursor, the COP surface was functionalized by VUV/(O)-modification in order to increase the adhesion between the precursor gel film and the COP surface. In the FTIR spectra of the VUV/(O)-modified COP substrate, the band at 3000-2800 cm^{-1} and peak at 1447 cm^{-1} were due to C-H stretching and deformation vibrations from the alkyl structures, respectively.[45,46] IR absorption bands at 1800-1600 cm^{-1} due to vibrations of oxygenated carbon species appeared after VUV/(O)-modification of the COP surface. FTIR spectra of the TAA gel films on the COP substrates showed similar IR absorption to the TAA gel films on the silicon substrates. After the TAA gel films were irradiated by VUV/(O), the acetylacetonate-related bands mostly disappeared, leaving the IR absorption bands corresponding to the spectra of the VUV/(O)-modified COP surface. Since the theoretical light penetration depth of ATR-mode FTIR measurement with a Ge prism is around 0.5 μm (light penetration depth: 0.66 μm in region of 1000 cm^{-1} and 0.44 μm in region of 1500 cm^{-1}),[47] we could not prevent the absorption bands of VUV/(O)-modified COP from overlapping with the TAA spectra. Despite this, removal of acetylacetonate groups from the

precursor gel films was confirmed by the spectra changes due to the VUV/(O)-treatment. After the acetylacetonate ligands were dissociated, the remained inorganic substances in the gel films, most likely titanium oxides, were further investigated by XPS to understand their chemical states.

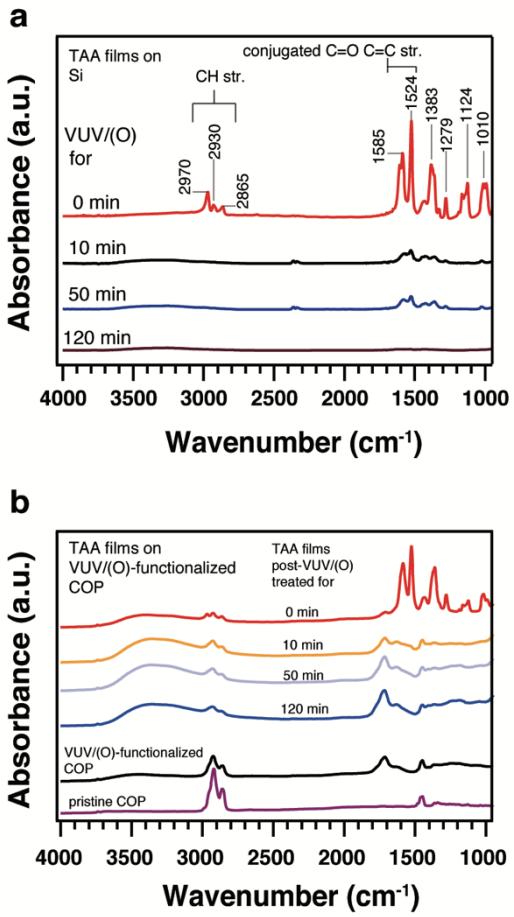

Figure 2. IR spectra of TAA gel films formed on (a) the Si substrates and (b) the COP substrates. The changes of IR bands were observed in various VUV/(O)-irradiation time.

2.2. Formation of TiO_2

To investigate the chemical states of the remained inorganic films, XPS measurements were carried out by acquiring C1s, O1s, Ti2p spectra, as shown in **Figure 3**. Deconvolution of the C1s spectra indicated that oxygenated carbon species corresponding to binding energies of ~284.8 eV for C–C, ~286.0 eV for C–O, ~287.2 eV for C=O and ~289.1 eV for O–C=O[48–50] were

clearly decreased by the VUV/(O)-treatment. These results are consistent with the results of FTIR. After VUV/(O)-treatment for 2 h, the peaks associated with the organic functional groups mostly disappeared. The residual C1s peak areas were due to contaminant adsorption during transferring the samples to the XPS instruments.[20,51,52] O1s spectra were deconvoluted into Ti–OH (~532.5 eV), O–C (~532.2 eV), O=C (~531.5 eV) and O–Ti(IV) (~530.4 eV).[20,53,54] The deconvoluted peaks of O=C and O–C vanished after 2 h VUV/(O)-treatment, and the peak intensity of O–Ti(IV) component increased. The changes in peak intensity are attributed to the dissociation of carbonyl groups and conjugated alkoxy groups, which are in good agreement with previously reported photo-generated metal oxide films.[20,55] Besides, we noticed a slight peak shift of ~0.2 eV in the deconvoluted peaks of O–Ti(IV), where the O–Ti(IV) peak in the as-spun TAA films centered at ~530.3 eV and the O–Ti(IV) peak in VUV/(O)-treated TAA films centered at ~530.5 eV. Such slight shifts have been also reported in another related study which produced TiO_2 by VUV/(O)-treatments.[20] We considered that the slight binding energy shifts in O–Ti(IV) appeared because the O–Ti bonds are in different chemical environments, *e.g.* chelate bonds between C=O to Ti and ionic bonds of O–Ti,[26,27] in the precursor TAA and in the inorganic TiO_2. However, so far it is difficult to give an appropriate explanation to such shifting without sufficient evidences. In the Ti2p spectra, the peak positions of $Ti2p_{1/2}$ and $Ti2p_{3/2}$ were at 464.6 eV and 458.8 eV respectively, which were assigned to Ti(IV) as previously reported.[20,56,57] After VUV/(O)-treatment, no obvious shifting of Ti2p was observed, which indicated that the titanium content in the VUV/(O)-treated gel films remained their oxidation state of Ti(IV) without generating any Ti(III) or metallic Ti. As a result, the VUV/(O)-treatment in ambient conditions successfully removed the organic moieties and form TiO_2 thin films.

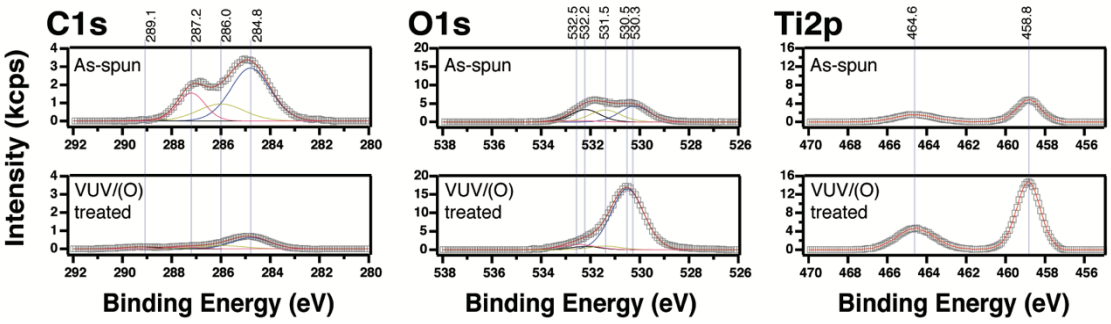

Figure 3. XPS spectra of C1s, O1s and Ti2p of TAA precursor thin films before and after VUV/(O)-treatment for 2h. Square markers represent the measured spectra. Red curves represent the envelopes of overlapping deconvolution peaks.

2.3. Characterizations of TiO_2 micropatterns

After investigating the formation of TiO_2 thin films on the silicon substrates and the COP substrates, we further performed TiO_2 micropatterning. We focused on developing TiO_2 micropatterning techniques on the COP substrates. Photomasks with striped and circular slits were used for VUV/(O) patterning. The TAA gel films were irradiated by VUV light transmitted through the slits of a photomask. Active oxygen species (O) were generated above the gel films at the VUV-irradiated regions, and these oxidative species participated in the dissociation of organics.[21] The irradiated regions were converted to TiO_2, while the precursor gels in the masked regions retained their acetylacetonate chelating structure, which were soluble in alcoholic solvents. After washing away the untreated TAA gels by 2-propanol solvent, well-defined striped and circular patterns were successfully formed over a large area, observed by optical microscope shown in **Figure 4**. SEM images of the TiO_2 striped and circular micropatterns are shown in **Figure 5**. EDX element mapping images illustrate the Ti element distribution corresponding to the SEM images, clearly verifying the removal of untreated TAA gels from the non-irradiated regions.

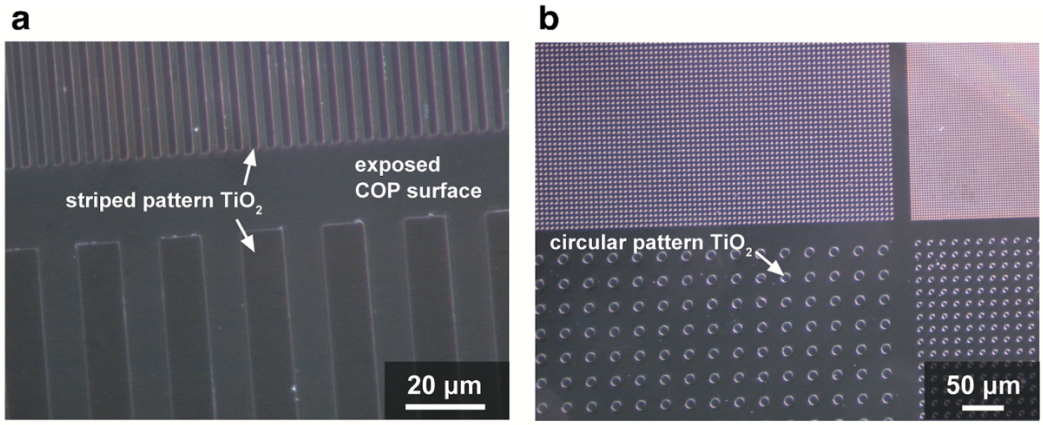

Figure 4. Optical images of the TiO_2 micropatterns on COP substrates. Optical images were observed by optical microscopy in dark field mode. (a) Striped micropatterns with widths of 2 μm and 10 μm (top to bottom). (b) circular micropatterns with diameters of 2 μm, 1 μm, 5 μm and 10 μm (clockwise from the top-left).

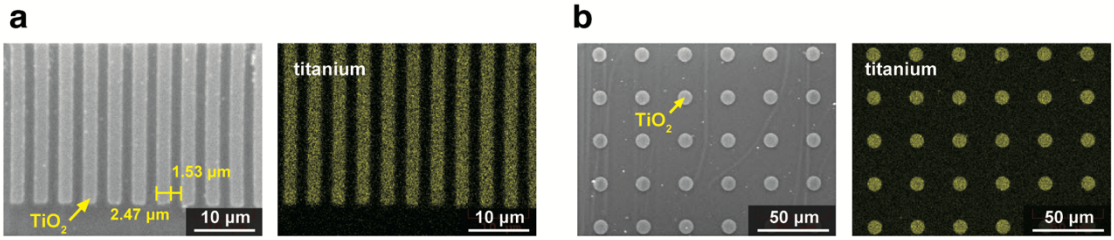

Figure 5. SEM images and EDX titanium element mapping images of (a) striped and (b) circular micropatterns on COP substrates. Clean removal of TAA precursor is confirmed by the titanium element mapping.

The line edge roughness of micropatterns is an important parameter when fabricating electronics.[17,18] Line edge roughness of the VUV/(O)-fabricated TiO_2 striped micropatterns was estimated by measuring the standard variations of line width. The SEM image (**Figure S2**) revealed an average line width of 11.0 μm with a standard variation of 0.34 μm in a nominal 10-μm-striped region, and an average line width of 2.47 μm with a standard variation of 0.09 μm in a nominal 2-μm-striped region. This corresponded to a line edge roughness of 3.1% (0.34/11) in the nominal 10-μm-striped patterns and 3.6% (0.09/2.47) in the nominal 2-μm-striped patterns. The average line width was slightly larger than the nominal width of the

photomask, most likely due to diffusion of the active oxygen species.[21,24] Nevertheless, a low value of line edge roughness was obtained in our method, which was lower than the usual variation of 5% in general electronic design. Moreover, this value is much more precise than the results of other TiO_2 micropatterning techniques at room temperature using LPD, *i.e.*, with hydrophilically-patterned SAM template (28%)[18] or hydrophilically-patterned polymer surface (17% by ultrasonic lift-off and 4.8% after further peeling by adhesive tape).[17]

Cross-sectional TEM images were obtained by slicing the sample perpendicularly to the 1-μm-striped TiO_2 patterns, as shown in **Figure 6**. The morphology of micropatterns was shown by STEM dark-field images (**Figure 6a**). A magnified image of one TiO_2 pattern is shown in the inset. Layers from the bottom to the top were the COP substrate, a TiO_2 pattern, a carbon coating for scanning ion microscope observation, and a phenanthrene ($C_{14}H_{10}$) protective film coated for the forced ion beam slicing process. They were represented as i., ii., iii. and iv., respectively. EDX element mapping images (**Figure 6b**, **c**) illustrate the elemental distributions of carbon and titanium. Titanium element exists only in the TiO_2 pattern regions, revealing the clean removal of TAA gels on the undesired regions. Carbon element exists abundantly in the COP substrate (i.) as well as the carbon coating (iii.) and the phenanthrene film (iv.). A deficiency of carbon element was found in the TiO_2 pattern regions, revealing a clear elimination of organics from the TAA gels by the VUV/(O)-treatment.

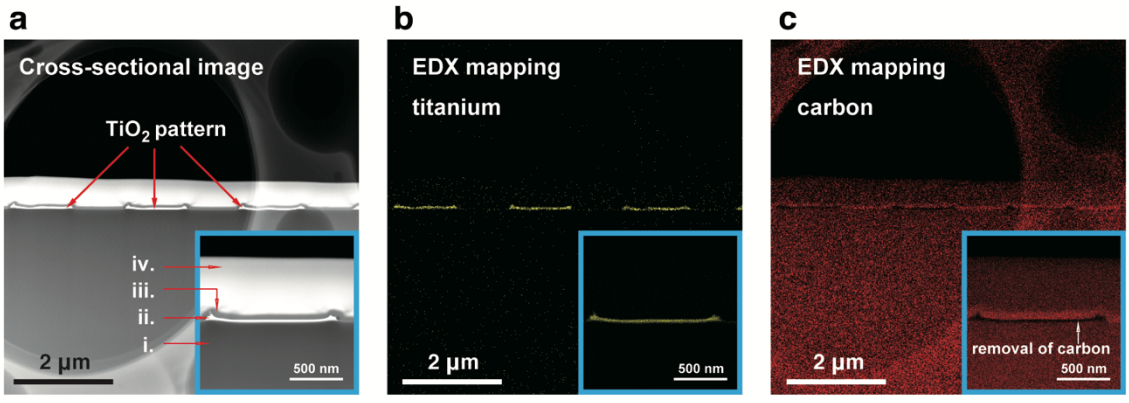

Figure 6. TEM cross-sectional images of 1-μm-striped TiO_2 patterns from a TAA solution of 0.05 mol/L on a COP substrate. (a) STEM dark field image. Inset shows the magnified image of one TiO_2 pattern. Each layer is represented as: i. COP substrate, ii. TiO_2 pattern, iii. carbon coating, iv. $C_{14}H_{10}$ protective film. (b) EDX element mapping of titanium. (c) EDX element mapping of carbon.

Although the prepared TiO_2 thickness from a TAA solution of 0.05 mol/L is short (~60 nm), we believe that by increasing the thickness of the spin-coated TAA gels, the thickness of the resulting TiO_2 patterns could be increased. For example, we spin-coated a "thicker" TAA solution with a double concentration (0.1 mol/L) on the COP substrates (the same parameter of rotation rates and time), and conducted VUV/(O)-patterning. The thickness of the resulting TiO_2 patterns increased to ~100 nm, as shown in **Figure S3**. However, such thickening still has its limitation. Amorphous TiO_2 films have a continuous and strong absorption band in the wavelength range of ultraviolet ($\lambda < 310$ nm).[31] Once the penetration of the VUV light ($\lambda = 172$ nm) and the permeation of active oxygen species reached the limit, the deeper TAA gel films out of this limit would not be converted to TiO_2. The present report is focusing on studying the feasibility of the TiO_2 micropatterning via VUV/(O) lithography, nevertheless, further studies could be devoted to investigation of thicker pattern formation for the demands of application.

Due to the whole ambient reaction conditions, our VUV/(O)-patterning strategy could be a general approach for TiO_2 patterning on arbitrary substrates, and the demonstrated patterning has a minimum feature of 1 μm. The photolithography is conducted by VUV light with a wavelength of 172 nm, the resolution of our TiO_2 patterning is essentially constrained by the optical resolution. Moreover, the broadening of the pattern widths due to the active oxygen species was also observed. These set a constrain for achieving higher resolution. In some other works about micropatterning using VUV-photolithography, the resolution could be achieved to

~500 nm.[46] We believe that our TiO_2 patterning technique with μm-scale resolution is satisfactory for the industrial application.

We determined the crystallinity of our VUV/(O)-fabricated TiO_2 micropatterns by HR-TEM (**Figure S4a**) and SAED (**Figure S4b**). Both HR-TEM and SAED images indicate that VUV/(O)-fabricated TiO_2 from TAA precursor was amorphous, similar to the result of the VUV/(O)-fabricated TiO_2 from titanium alkoxide precursors.[20] VUV-obtained metal oxides were reported to be amorphous.[19,20] However, as mentioned in the introduction part, several reported photo-crystallization strategies can be combined with our VUV/(O)-patterning method to produce crystalline TiO_2 patterns. Also, our amorphous TiO_2 patterns revealed their potentials as components for sensors,[32] resistive random access memories,[33–36] solar cell elements[37,38] and photovoltaic materials.[39] Moreover, amorphous TiO_2 also attracted attention by demonstrating its photo-activities.[40,41] In the next section, we demonstrate photo-metallization of copper on the amorphous TiO_2 patterns to form metal patterns.

2.4. Selective Cu deposition on TiO_2 micropatterns

Direct photo-deposition of copper on patterned TiO_2 nanocrystals was already reported to form conductive circuit patterns on dielectric substrates.[58] Our VUV/(O)-fabricated TiO_2 micropatterns can also be applied to the site-selective deposition of copper metal through their photocatalytic activities. Low-molecular-weight alcohols such as methanol and ethanol are widely used as hole scavengers. In this work, we used 3:1 methanol/ethanol by volume as both the solvent and the hole scavenger for the photo-deposition experiments. Nitrogen purging during the photo-deposition reaction was utilized to remove dissolved oxygen from the solvent. UV-Vis transmission spectra of the copper acetate methanol/ethanol solution, as shown in **Figure S5**, revealed that sufficient photons for excitation were able to reach the TiO_2-patterned substrate at the solution thickness of 0.4 mm (transmittance of *ca*. 60% at 248 nm and above

80% in the range of 300 nm - 500 nm). In the SEM-EDX image (**Figure 7a, b, c**), copper signal was detected only on the TiO_2 micropatterns, indicating that copper was deposited only on the TiO_2 micropatterns. The shapes and sizes of TiO_2 patterns before and after the photocatalytic copper deposition were observed, as shown in **Figure S6**. Here we compared the copper deposited TiO_2 (Cu/TiO_2) patterns with diameters of 5 μm to the as-prepared TiO_2 patterns with diameters of 5 μm. EDX element mapping was shown corresponding to the SEM images. The diameters of patterns of each element in EDX images were measured to evaluate the change in size. The diameter of the as-prepared TiO_2 patterns (Ti element) was measured to be 5.0 ± 0.1 μm. In the images of the Cu deposited patterns, Cu patterns (Cu element) have a diameter of 5.1 ± 0.3 μm, where the diameter of TiO_2 patterns beneath them (Ti element) is 5.0 ± 0.2 μm. After the photocatalytic copper deposition, TiO_2 patterns retained the circular shape and the diameters. The diameter of the Cu patterns was slightly larger than the diameter of TiO_2 patterns, most likely due to the growth of the deposited copper. Nevertheless, all the element mapping patterns retained the circular shape and revealed good consistency to the patterns of the photomask.

XPS measurements were conducted to understand the chemical composition of the Cu deposited TiO_2 patterns on the COP substrates, as shown in **Figure 7d**. $Cu2p_{3/2}$ spectra show a main peak at 932.9 eV, and there is no Cu^{2+} satellite at 944-941 eV, indicating that Cu(II) species no longer existed after photo-deposition. The deposited Cu should be the reduced species such as copper metal or cuprous oxide (Cu_2O). A weak satellite peak at ~945 eV was detected, which is usually attributed to Cu_2O.[59] However, since the XPS photoelectron signals are sensitive on the very surface, to understand the chemical states of Cu within the copper deposition, other characterization *i.e.* HR-TEM and SAED should be conducted, which will be discussed later. Ti2p spectra show a slightly swelled signal centered at 464.8 eV indicative of $Ti2p_{1/2}$ and a relevantly stronger $Ti2p_{3/2}$ peak at 459.1 eV. The weak intensity of these Ti2p photoelectron signals indicated that the TiO_2 patterns were embedded by the Cu deposition. Such weakening

of the intensity of Ti2p signals was also reported in the related studies.[58] C1s spectra show a sharp peak of C–C at 285 eV with a shoulder at 290-286 eV. These peak can be attributed to the VUV/(O)-modified COP surface where the regions were not covered by the Cu/TiO_2 patterns.[45] O1s spectra show a main peak centered at 530.8 eV and a subpeak at 533-532 eV. The subpeak at 533-532 eV was attributed to oxygenated carbon groups from the VUV/(O)-modified COP surface.[45,53] The peak centered at 530.8 eV is usually attributed to metal oxides: here the metal oxides should be TiO_2 and naturally formed cuprous oxide on the deposited copper metal.[54,59] Overall, the SEM-EDX and XPS results indicated that Cu was successfully deposited on the TiO_2 patterns. More detailed information about the crystallinity of deposited Cu and TiO_2 was investigated by TEM.

The HR-TEM image of deposited Cu (**Figure 8a**) shows clearly well-crystallized copper species with interplanar distance of 2.10 Å corresponding to Cu(111), referenced to ICDD-JCPDS data base (face center cubic copper, JCPDS card No. 04-0836). Also, the HR-TEM image of the boundary region between TiO_2 and Cu is shown in **Figure 8b**. In the Cu region, well-crystallized structures with interplanar distance of 2.10 Å were also observed, which corresponded to Cu(111). In the TiO_2 region, the structure retained amorphous even after the UV irradiation from the high-pressure mercury lamp for 1 h. Selective area electron diffraction (SAED) patterns were acquired from the Cu region and from the TiO_2 region. SAED image of the TiO_2 region (**Figure 8c)** shows a non-crystalline result. On the contrary, SAED image of the Cu region (**Figure 8d)** shows that the lattice spacings of 2.10 Å, 1.83 Å, 1.31 Å, 1.11 Å, 0.86 Å, which are attributed to copper metal: Cu(111), Cu(200), Cu(220), Cu(311), Cu(331), respectively (referenced to JCPDS card No. 04-0836). Crystal structures of either cuprous oxide or cupric oxide were not observed by SAED measurements. These proved that the deposited Cu was copper metal. O1s photoelectron signals at 530.8 eV and Cu2p satellite at 945 eV might be attributed to naturally formed amorphous cuprous oxide due to the exposure in air.[59] Accordingly, a patterning of copper metal on the VUV/(O)-fabricated TiO_2 micropatterns was

successfully demonstrated. This method can also be applied to other precious metals, *e.g.* Au, Ag, Pd.[60-62] By using the VUV/(O)-fabricated TiO_2 micropatterns, surface processing techniques for pattern formation of metals on polymer substrates can be simply achieved, which raise interesting possibilities for the new design and creation of flexible electronic and optoelectronic devices.

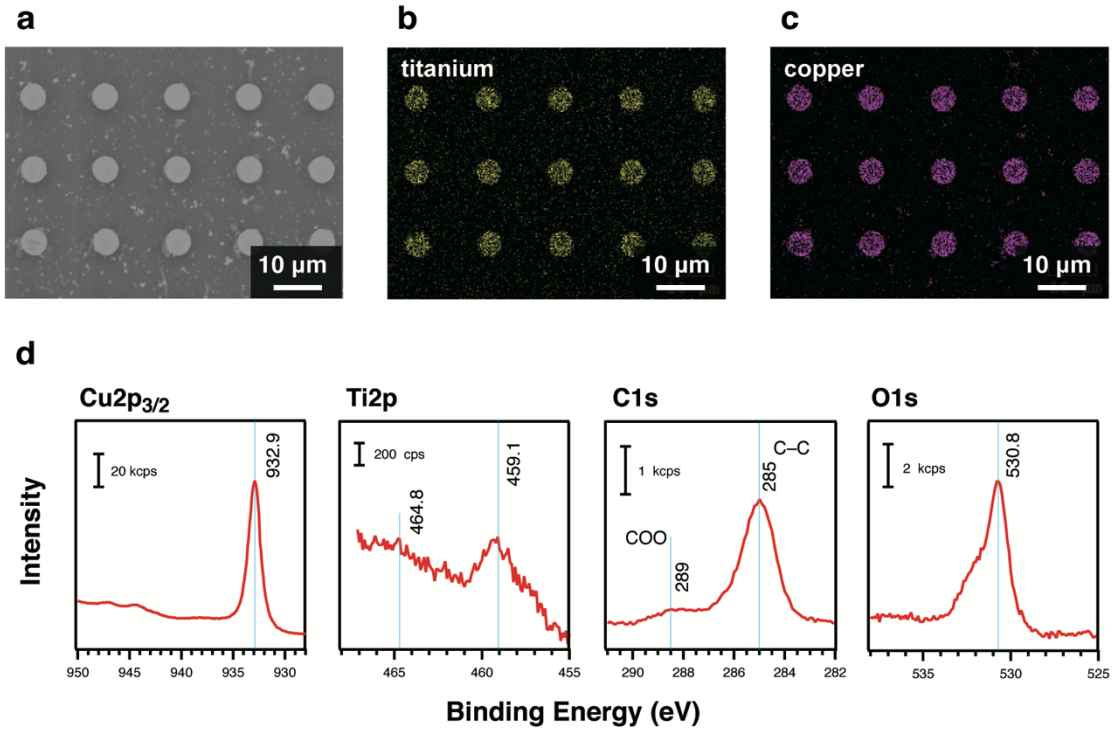

Figure 7. Photo-deposition of copper on TiO_2 micropatterns by UV-irradiation through a copper acetate solution. SEM image of TiO_2 circular patterns on a COP substrate after photo-deposition: (a) SEM image and its corresponding EDX element mapping images of (b) titanium and (c) copper. (d) Chemical states of the resulting Cu deposited patterns on the COP substrates, studied by XPS spectra $Cu2p_{3/2}$, Ti2p, C1s, O1s.

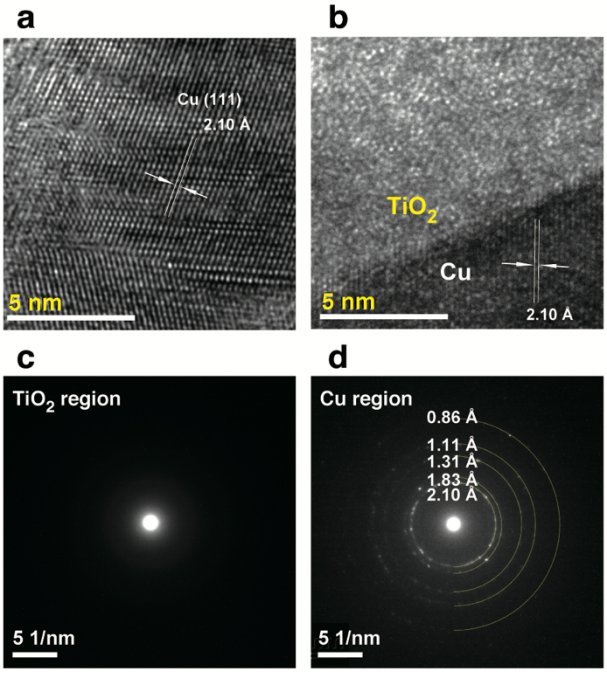

Figure 8. HR-TEM images and SAED patterns of the resulting Cu deposited patterns. (a) HR-TEM image of the Cu region. (b) HR-TEM image of the boundary region between TiO_2 and Cu. (c) SAED pattern from the TiO_2 region. (d) SAED pattern from the Cu region.

3. Conclusion

We have demonstrated a microfabrication method for a large-area patterning of TiO_2 on a polymer substrate, which could be fully conducted in an ambient environment. TAA was proved to be a favorable precursor due to its chemical stability in ambient air, and it thus played a key role in further patterning processes, in which the untreated precursor gels on the undesired regions can be cleanly removed. VUV/(O)-treatment eliminated the organic moieties from the TAA precursor gel films and formed TiO_2 thin films. Well-defined amorphous TiO_2 micropatterns with a minimum feature of 1 μm were fabricated by VUV/(O)-treatment through a photomask. Since neither heat-treatments nor other severe conditions were required, this method is well suited for pattern fabrication on polymer substrates. High-quality amorphous

TiO_2 micropatterns are useful in electronics, memories, solar cells, sensors, as well as photocatalysis used to form metal arrays. Some previously reported photo-crystallization techniques provided opportunities to convert our amorphous TiO_2 micropatterns into rutile, therefore, these TiO_2 patterns could meet a wider range of requirements of electronics fabrication. Further studies should be devoted to developing one-step patterning and crystallizing techniques. Overall, our VUV/(O) patterning technique proves to be a simple, precise and cost-effective TiO_2 patterning technique, and we believe that it will lead to future synthesis approaches for device fabrication on flexible polymer substrates.

4. Experimental Section

VUV oxidative treatments: A Xe_2 excimer lamp (λ = 172 nm, UER 20-172V, Ushio Inc.) was used for a VUV irradiation. The power of irradiation was measured to be 10 $mW \cdot cm^{-2}$ with an irradiation distance of 5 mm in nitrogen-filled chamber. The VUV oxidative treatment was performed in an ambient condition, thus VUV light and generated active oxygen species (VUV/(O)) participated in the photochemical reaction. The irradiation distance was fixed to 5 mm.

Preparation of substrates: A COP (ZF16-188, thickness of 188 μm, ZeonorFilm®, Zeon Corporation) sheet was cut into 2 cm × 2 cm pieces, the protective films were peeled off, and the VUV/(O)-modification for 50 min was performed to functionalize the surface. A non-doped Si(100) wafer (thickness of 525±25 μm with resistance of $\geqq$1000 Ω·cm, Electronics & Materials Co. Ltd) was cut to 2 cm x 2 cm, then sonicated in ethanol (99.5%, Nacalai Tesque) and in ultrapure water (UPW) for 20 min each. The silicon substrate was then VUV/(O)-treated for 20 min in order to remove adsorbed organic impurities and to activate the surface.

Precursor gel film and its chemical stability in air: A solution of 0.1 mol/L TAA was prepared by diluting commercial TAA solution [63% (w/w) in 2-propanol, Tokyo Chemical Industry(TCI)] with 2-propanol (99%, Nacalai Tesque). Spin-coating was performed using a solution drop of 100 μL at 500 rpm for 15 s followed by 2000 rpm for 100 s. TAA gel films were formed on the COP substrates or the silicon substrates. Time-dependent chemical changes of the spun gel films in ambient air were observed by FTIR.

Formation of TiO_2 thin films: The spun TAA gel films on the COP substrates or the silicon substrates were VUV/(O)-treated for a series of irradiation time. The chemical compositions of VUV/(O)-treated TAA gel films were characterized by FTIR and XPS.

TiO_2 micropatterning on polymer substrates: TAA gel films on the COP substrates were prepared as previously described, which used TAA with concentration of 0.05 mol/L and 0.1 mol/L. A photomask (chromium patterns 100 nm in thickness on a 2-mm-thick quartz plate; light transparency of 93% at 172 nm) was used for micropatterning. After the irradiation, the substrates were rinsed in 2-propanol to remove the TAA gel film at the masked regions. The resulting TiO_2 micropatterns were characterized by optical microscopy, scanning electron microscopy and energy-dispersive X-ray spectrometry (SEM-EDX), and transmission electron microscopy (TEM).

Site-selective deposition of copper metal on TiO_2 micropatterns: A solution of 0.25 mmol/L copper acetate was prepared by dissolving copper acetate monohydrate powder (>95%, TCI) into a methanol/ethanol (vol. ratio 3:1) mixed solution. The substrate with TiO_2 micropatterns was immersed into the copper acetate solution in a quartz photochemical cell, and it was irradiated by a high-pressure mercury lamp (REX-250, Asahi spectra) at 200 $mW \cdot cm^{-2}$ for 1 hour with purging N_2. UV light propagated through the copper acetate methanol/ethanol solution (thickness of ~0.4 mm) and reached the TiO_2 patterns. To quantify the effective irradiation, UV-Vis transmittance measurement in the copper acetate methanol/ethanol solution was conducted using a UV-Vis spectrometer (U-3500, Hitachi). Afterward, the substrate was

rinsed in UPW in order to remove copper acetate remaining on the surface. Selective photo-deposition of copper was characterized by XPS and SEM-EDX.

Characterization: FTIR (Excalibur FTS-3000, Digilab) was utilized for monitoring the changes in organic moieties of TAA during the VUV/(O)-induced photochemical conversion by applying transmission-mode or attenuated total reflection mode (ATR-mode). ATR-mode FTIR measurement was carried out using a grazing angle attenuated total reflectance Ge crystal with a reflection angle of 65º. All the measurements were conducted in an ambient environment, and the IR spectra were taken in the range of 4000-950 cm^{-1} with a resolution of 2 cm^{-1}. XPS and Auger spectra were received by a photoelectron spectrometer (JPS-9010TRX, JEOL) equipped with a Mg K_{α} X-ray source (emission current 10 mA, accelerate voltage 10 kV) in a highly-evacuated environment (10^{-7} - 10^{-6} Pa) to study the chemical changes. High resolution spectra of O1s, Ti2p, C1s, Cu2p were recorded at each energy step of 0.1 eV. The obtained XPS spectra were referenced to C-C at 285.0 eV. AFM (MFP-3D, Oxford Instruments) was used to visualize the morphology of TiO_2 micropatterns in AC dynamic mode using aluminum backside-coated Si probes (SI-DF-40, Hitachi Hi-Tech Co. Ltd.). The measurements were performed in an ambient environment. Prior to the SEM observation, a conductive carbon film was coated on the samples by a high vacuum evaporator (HUS-5GB, Hitachi). The micrographs and the corresponding element mapping images of TiO_2micropatterns were received by a SEM-EDX facility (SEM: S-3500H, Hitachi; EDX: Delta Plus 3, Kevex/Fisons Instruments Inc.). The measurements were conducted at an acceleration voltage of 15 kV. Sliced samples for TEM cross-section images were prepared by the focused ion beam (FIB) cutting technique with a scanning ion microscope (SIM), using a finely-focused beam of gallium ions (JFIB-2300, JEOL). Prior to the cutting, a phenanthrene ($C_{14}H_{10}$) protective film with a depth of ~1 μm was coated on the sample. TEM (JEM-2100F, JEOL) measurements were performed at an acceleration voltage of 200 kV to investigate the cross-section images and element distributions of micropatterns by applying scanning TEM (STEM) and TEM-EDX. The crystallinity of TiO_2

and photo-deposited copper were studied using high resolution TEM (HR-TEM) and selected area electron diffraction (SAED). The electron diffraction patterns and interplanar distances were compared to the ICDD-JCPDS database, where Cu (JCPDS card No. 04-0836), Cu_2O (JCPDS card No. 05-0667), CuO (JCPDS card No. 80-1916) are referenced.

Supporting Information

Supporting Information is available from the Wiley Online Library or from the author.

Acknowledgements

This work was partially supported by JSPS KAKENHI grant number JP15H02297. Cheng-Tse Wu acknowledges Ms. Chiao-Ying Chien for useful scientific advice.

Received: ((will be filled in by the editorial staff))
Revised: ((will be filled in by the editorial staff))
Published online: ((will be filled in by the editorial staff))

References

[1] A. L. Linsebigler, G. Lu, J. T. Yates, *Chem. Rev.* **1995**, *95*, 735.

[2] R. Mechiakh, F. Meriche, R. Kremer, R. Bensaha, B. Boudine, A. Boudrioua, *Opt. Mater. (Amst).* **2007**, *30*, 645.

[3] H. Tang, K. Prasad, R. Sanjinès, P. E. Schmid, F. Lévy, *J. Appl. Phys.* **1994**, *75*, 2042.

[4] M. G. B O'regan, *Nature* **1999**, *353*, 737.

[5] I. Valitova, P. Kumar, X. Meng, F. Soavi, C. Santato, F. Cicoira, *ACS Appl. Mater. Interfaces* **2016**, *8*, 14855.

[6] Q. Li, A. Khiat, I. Salaoru, H. Xu, T. Prodromakis, *Nanoscale Res. Lett.* **2014**, *9*, 1.

[7] D. Chen, Y. Gao, G. Wang, H. Zhang, W. Lu, J. Li, *J. Phys. Chem. C* **2007**, *111*, 13163.

[8] J. H. Park, S. Kim, A. J. Bard, *Nano Lett.* **2006**, *6*, 24.

[9] A. S. Zuruzi, N. C. MacDonald, *Adv. Funct. Mater.* **2005**, *15*, 396.

[10] A. S. Zuruzi, A. Kolmakov, N. C. MacDonald, M. Moskovits, *Appl. Phys. Lett.* **2006**, *88*, 102904.

[11] M. H. Suhail, G. M. Rao, S. Mohan, *J. Appl. Phys.* **1992**, *71*, 1421.

[12] P. Chrysicopoulou, D. Davazoglou, C. Trapalis, G. Kordas, *Thin Solid Films* **1998**, *323*, 188.

[13] N. Rausch, E. P. Burte, *J. Electrochem. Soc.* **1993**, *140*, 145.

[14] S. Park, G. Wang, B. Cho, Y. Kim, S. Song, Y. Ji, M. Yoon, T. Lee, *Nat. Nanotechnol.* **2012**, *7*, 438.

[15] J.-G. Yu, H.-G. Yu, B. Cheng, X.-J. Zhao, J. C. Yu, W.-K. Ho, *J. Phys. Chem. B* **2003**, *107*, 13871.

[16] A. Dutschke, C. Diegelmann, P. Löbmann, *J. Mater. Chem.* **2003**, *13*, 1058.

[17] P. Yang, M. Yang, S. Zou, J. Xie, W. Yang, *J. Am. Chem. Soc.* **2007**, *129*, 1541.

[18] K. Koumoto, S. Seo, T. Sugiyama, W. S. Seo, W. J. Dressick, *Chem. Mater.* **1999**, *11*, 2305.

[19] Y. Naganuma, S. Tanaka, C. Kato, *Jpn. J. Appl. Phys.* **2004**, *43*, 6315.

[20] P. C. With, U. Helmstedt, S. Naumov, A. Sobottka, A. Prager, U. Decker, R. Heller, B. Abel, L. Prager, *Chem. Mater.* **2016**, *28*, 7715.

[21] Y. Tu, T. Utsunomiya, T. Ichii, H. Sugimura, *ACS Appl. Mater. Interfaces* **2016**, *8*, 10627.

[22] T. Utsunomiya, T. Kanzawa, T. Ichii, H. Sugimura, *Thin Solid Films* **2017**, *638*, 28.

[23] A. I. A. Soliman, T. Utsunomiya, T. Ichii, H. Sugimura, *Langmuir* **2018**, *34*, 3228.

[24] O. P. Khatri, H. Sano, K. Murase, H. Sugimura, *Langmuir* **2008**, *24*, 12077.

[25] A. Hozumi, T. Masuda, H. Sugimura, *Langmuir* **2003**, *19*, 7573.

[26] N. Tohge, K. Shinmou, T. Minami, *J. Sol-Gel Sci. Technol.* **1994**, *2*, 581.

[27] M. Krunks, I. Oja, K. Tõnsuaadu, M. Es-Souni, M. Gruselle, L. Niinisto, *J. Therm. Anal. Calorim.* **2005**, *80*, 483.

[28] Y. S. Rim, H. Chen, Y. Liu, S. H. Bae, H. J. Kim, Y. Yang, *ACS Nano* **2014**, *8*, 9680.

[29] H. Tsuchiya, J. M. Macak, A. Ghicov, A. S. Räder, L. Taveira, P. Schmuki, *Corros. Sci.* **2007**, *49*, 203.

[30] T. Tsuchiya, A. Watanabe, Y. Imai, H. Niino, I. Yamaguchi, T. Manabe, T. Kumagai, S. Mizuta, *Japanese J. Appl. Physics, Part 2 Lett.* **1999**, *38*, 823.

[31] G. Krylova, C. Na, *J. Phys. Chem. C* **2015**, *119*, 12400.

[32] H. F. Lu, F. Li, G. Liu, Z. G. Chen, D. W. Wang, H. T. Fang, G. Q. Lu, Z. H. Jiang, H. M. Cheng, *Nanotechnology* **2008**, *19*, 1.

[33] H. Y. Jeong, J. Y. Lee, S. Y. Choi, *Adv. Funct. Mater.* **2010**, *20*, 3912.

[34] H. Young Jeong, S. Kyu Kim, J. Yong Lee, S. Y. Choi, *J. Electrochem. Soc.* **2011**, *158*, 979.

[35] H. Y. Jeong, S. K. Kim, J. Y. Lee, S. Y. Choi, *Appl. Phys. A Mater. Sci. Process.* **2011**, *102*, 967.

[36] L. Zou, W. Hu, W. Xie, R. Chen, N. Qin, B. Li, D. Bao, *Appl. Surf. Sci.* **2014**, *311*, 697.

[37] Z. Ren, J. Wang, Z. Pan, K. Zhao, H. Zhang, Y. Li, Y. Zhao, I. Mora-Sero, J. Bisquert, X. Zhong, *Chem. Mater.* **2015**, *27*, 8398.

[38] A. Kogo, Y. Sanehira, Y. Numata, M. Ikegami, T. Miyasaka, *ACS Appl. Mater. Interfaces* **2018**, *10*, 2224.

[39] I. S. Kim, R. T. Haasch, D. H. Cao, O. K. Farha, J. T. Hupp, M. G. Kanatzidis, A. B. F. Martinson, *ACS Appl. Mater. Interfaces* **2016**, *8*, 24310.

[40] Y. Gao, Y. Masuda, K. Koumoto, *Langmuir* **2004**, *20*, 3188.

[41] Z. Zhang, P. A. Maggard, *J. Photochem. Photobiol. A Chem.* **2007**, *186*, 8.

[42] K. Nakamoto, P. J. McCarthy, A. Ruby, A. E. Martell, *J. Am. Chem. Soc.* **1961**, *83*, 1066.

[43] J. Madarász, S. Kaneko, M. Okuya, G. Pokol, *Thermochim. Acta* **2009**, *489*, 37.

[44] J. Y. Zhang, I. W. Boyd, *Solid. State. Electron.* **1999**, *43*, 1107.

[45] Y. J. Kim, Y. Taniguchi, K. Murase, Y. Taguchi, H. Sugimura, *Appl. Surf. Sci.* **2009**, *255*, 3648.

[46] C. Wu, A. I. A. Soliman, T. Utsunomiya, T. Ichii, H. Sugimura, *RSC Adv.* **2019**, *9*, 32313.

[47] N. De Geyter, R. Morent, C. Leys, *Surf. Interface Anal.* **2008**, *40*, 608.

[48] A. I. A. Soliman, T. Utsunomiya, T. Ichii, H. Sugimura, *Appl. Surf. Sci.* **2017**, *416*, 971.

[49] R. Lapuente, C. Quijada, F. Huerta, F. Cases, J. L. Vázquez, *Polym. J.* **2003**, *35*, 911.

[50] D. H. Wang, Y. Hu, J. J. Zhao, L. L. Zeng, X. M. Tao, W. Chen, *J. Mater. Chem. A* **2014**, *2*, 17415.

[51] E. McCafferty, J. P. Wightman, *Surf. Interface Anal.* **1998**, *26*, 549.

[52] A. I. A. Soliman, T. Utsunomiya, T. Ichii, H. Sugimura, *Langmuir* **2018**, *34*, 13162.

[53] J. P. Boudou, J. I. Paredes, A. Cuesta, A. Martinez-Alonso, J. M. D. Tascon, *Carbon N. Y.* **2003**, *41*, 41.

[54] X. Sun, M. Xie, G. Wang, H. Sun, A. S. Cavanagh, J. J. Travis, S. M. George, J. Lian, *J. Electrochem. Soc.* **2012**, *159*, A364.

[55] Y. H. Kim, J. S. Heo, T. H. Kim, S. Park, M. H. Yoon, J. Kim, M. S. Oh, G. R. Yi, Y. Y. Noh, S. K. Park, *Nature* **2012**, *489*, 128.

[56] J. Park, T. Back, W. C. Mitchel, S. S. Kim, S. Elhamri, J. Boeckl, S. B. Fairchild, R. Naik, A. A. Voevodin, *Sci. Rep.* **2015**, *5*, 1.

[57] Z. Wang, U. Helmersson, P. O. Käll, *Thin Solid Films* **2002**, *405*, 50.

[58] K. Akamatsu, A. Kimura, H. Matsubara, S. Ikeda, H. Nawafune, *Langmuir* **2005**, *21*, 8099.

[59] I. Platzman, R. Brener, H. Haick, R. Tannenbaum, *J. Phys. Chem. C* **2008**, *112*, 1101.

[60] X. Li, Y. Tian, P. Xia, Y. Luo, Q. Rui, *Anal. Chem.* **2009**, *81*, 8249.

[61] S. Nishimoto, A. Kubo, X. Zhang, Z. Liu, N. Taneichi, T. Okui, T. Murakami, T. Komine, A. Fujishima, *Appl. Surf. Sci.* **2008**, *254*, 5891.

[62] C. E. J. Cordonier, H. Endo, T. Kagami, Y. Okabe, M. Ide, S. Suzuki, H. Honma, *J. Electrochem. Soc.* **2013**, *161*, D1.

Table of Contents Entry
A one-step VUV treatment applied on TAA gel films directly generates TiO_2 micropatterns on polymer substrates in the whole ambient conditions. Deliberate processes such as glovebox and heat treatments are no longer needed. EDX element mappings reveal clear removal of untreated precursor gels from the undesired regions, which leads to high-quality inorganic TiO_2 patterns.

Keyword
Titanium dioxide; 172 nm Vacuum-ultraviolet; Photochemistry; Titanium acetylacetonate; Micropatterning

Authors
Cheng-Tse Wu. Author 1,
Ahmed I. A. Soliman. Author 2, Yudi Tu. Author 3, Toru Utsunomiya. Author 4, Takashi Ichii. Author 5, Hiroyuki Sugimura. Corresponding Author*

Title
Fabrication of TiO_2 Micropatterns on Flexible Substrates by Vacuum-ultraviolet Photochemical Treatments

ToC figure
(110 mm × 20 mm)